On the electronic improvement of multi-crystalline silicon via gettering and hydrogenation

J. Tan, A. Cuevas, D. Macdonald

Department of Engineering, College of Engineering and Computer Science, Australian National University, Canberra, ACT 0200, Australia

T. Trupke, R. Bardos

Centre of Excellence for Advanced Silicon Photovoltaics and Photonics, University of New South Wales, Sydney 2052, Australia..

K. Roth

Roth and Rau AG, Gewerbering 09337 Hohenstein-Ernstthal,OT Wuestenbrand, Germany

The electronic properties of multi-crystalline silicon must be improved during solar cell fabrication if highly efficient devices are to be made. This work shows how gettering and silicon nitride induced hydrogenation improve three properties: carrier lifetime, interstitial iron concentration and trap density. Area averaged effective carrier lifetimes less than 10μs were improved to greater than 60μs. A tenfold reduction in trap densities was achieved. Photoluminescence images showing the influence processing techniques have on the electronic properties of the silicon are presented.

Introduction

Most solar cells today are produced with a multi-crystalline silicon (mc-Si) substrate. This substrate is inherently defect and impurity rich, but excellent efficiencies can still be obtained.[1,2,3] This work investigates what improvements are made to the substrate during typical solar cell processing that allows these defect and impurity rich substrates to be manufactured into highly efficient solar cells. Phosphorus gettering has been studied for many years and is widely acknowledged to be vital in transforming the low minority carrier lifetimes of the typical mc-Si wafer.[4,5] Amorphous silicon nitride (SiN) thin films are a newer technology being widely adopted by industry as it strives to create more efficient solar cells. The passivation benefits that annealed SiN can bring are not as well understood as the gettering process and it is the combination of these two passivation effects that this paper addresses.

Experimental Design

A five inch p-type 1.6Ωcm (nominal) mc-Si brick fabricated by Deutsche Solar, was divided into six evenly spaced groups of wafers. Adjacent wafers from these sections were sorted into three sets of samples. The first series of wafers were alkaline etched and set aside as controls. These wafers will hence be referred to as "As-Cut". The remaining two sets received an alkaline etch prior to a 30min double sided phosphorus diffusion resulting in a sheet resistance of ~75Ω/□. One of the diffused sets was then acid etched to remove the n^+ emitter and thereby enable characterization of the bulk lifetime. These wafers will hence be referred to as "Gettered". The second diffused set retained its n^+ emitter and was reserved for characterization post SiN deposition and annealing. This series will be referred to as "Gettered + Hydrogenated". An industrial PECVD SiN film was deposited on all wafers using a Roth&Rau SiNA. System diagrams and descriptions of similar systems can be found in the literature.[6] "Gettered + Hydrogenated" samples were then annealed in a rapid thermal annealing furnace with peak temperatures of 700ºC and 800ºC which were held for 3s. Wafers were

then HF dipped to remove the fired SiN film, and acid etched before a fresh SiN was deposited (using an Oxford PlasmaLab 80+ system) to ensure uniform surface passivation. The photoconductance was measured at nine separate points across the sample using QSSPC.[7] Three parameters were studied: trap density, interstitial iron concentration [Fe_i] and effective lifetime at an excess carrier concentration of $1x10^{15}$ (τ_{eff}). Photoluminescence (PL) images of the samples were taken under approx. 1Sun illumination intensity.[8]

Results and Discussion

Carrier trapping is a phenomenon that frequently occurs in lifetime measurements taken at low injections levels on mc-Si substrates. The mechanism by which trapping occurs in mc-Si was explained by Macdonald and Cuevas[9] using a model from the 1950's[10]. Recent work has linked trapping to regions of high dislocation density and poor lifetime[9,11,12,13,18] and is increasingly being accepted as a good indicator of crystal quality. Recent research[14] indicates that these traps can be passivated by annealing SiN, which is confirmed by our data. Fig. 1 shows the influence that processing has on trap density. The shape of the control data is similar to that seen in the control [Fe_i] data (Fig. 2) and is related to the segregation of impurities during the solidification of the Si during casting. Though the distribution of Fe_i and trapping centres across the ingot maybe driven by the same mechanism, it is unlikely that Fe_i is a major trap centre. This is illustrated by the large difference in the magnitudes of [Fei] and trap density. After gettering we observe a high uniform trap concentration across the length of the brick. It is possible that the high temperatures required for phosphorus diffusion has created more traps, while simultaneously gettering some of the more lifetime degrading fast diffusing impurities such as Fe_i.[19] The gettered and hydrogenated data shown in Fig. 1, is an average of measurements taken for both annealing temperatures. Globally we observe a decrease of up to one order of magnitude in the trap density across the ingot after annealing the PECVD SiN. This decrease is attributed to hydrogenation of the defects which create traps.

Fig. 2 displays the reduction in [Fe_i] that processing can achieve on mc-Si wafers. The iron concentrations were determined following the methodology published by Macdonald *et al*.[15] The profile of the control samples is similar to what was observed in the control trap data from Fig. 1 and is consistent with previously published results.[16] Gettering has significantly decreased the [Fe_i] at both the top and bottom of the ingot with smaller changes in the middle positions. The "Gettered + Hydrogenated" samples at the top of the brick, show a small reduction in the [Fe_i], compared to their "Gettered" only counterparts. It is possible that hydrogenation of the samples during firing has reduced the [Fe_i]. However due to increased errors in the quantitative determination of the [Fei] when using this technique with samples of non-homogenous carrier lifetimes[20] (as is such for mc-Si wafers), this result does not strongly reinforces results published by Azzizi *et al.*[17] and Henze et al.[21], whom have shown that hydrogenation from annealed SiN films can passivate the deep level defect that Fe_i produces in the silicon band gap.

Ultimately the most important parameter that determines the efficiency of any solar cell is the carrier lifetime. Fig. 3 shows that gettering is effective at improving the τ_{eff} across all regions of the brick. The shape of the gettered τ_{eff} curve is the inverse of the [Fe_i] curve observed in Fig. 2, with the peak in τ_{eff} matching the lowest [Fe_i]. It is interesting to note that the flat region of lifetime at the top of the ingot matches well with the relatively flat [Fe_i] despite the preferential segregation of contaminants during ingot solidification which would increase the concentration of impurities in this region of the brick.[16] This would imply that the gettering was very effective at removing the high impurity concentration expected in this region. In general the annealed samples display an improved τ_{eff} in the higher regions of the brick due to bulk defect passivation from the annealed SiN. No temperature dependence was observed in the annealed samples as both 700ºC and 800ºC anneals seem to have increased the τ_{eff} to the same level.

The PL images in Fig. 4 are the central 30mm^2 regions of neighbouring wafers, from the top of the brick, after different processing treatments. The sampling time was kept constant at 1s. The area

averaged (~20mm^2) lifetime displayed with each image is the corresponding QSSPC measurement taken for that region of the wafer. Optical artefacts caused by texturing can be ignored as the samples were acid etched, which essentially leaves a planar surface. Figure 4 has been presented as a function of count rate. The PL count rate is directly proportional to the effective lifetime of the wafer. The lower count rate grains observed in Fig. 4a are not thought to be affected by their differing grain orientation. If grain orientation did affect the PL images, the darker grains in Fig. 4a would be consistently darker in Figs. 4b and 4c, which is not the case.

The image of the as-cut wafer (Fig. 4a) is remarkable in its clarity. The sharp definition of each grain, its boundaries and any scratches on the surface of the wafers (Fig. 4a, lower left hand corner) make this image comparable to a black and white photo of the sample. Despite the low τ_{eff}, reflected in the low maximum count rate, the image shows that there are some small differences in the electronic properties of the grains. Though grain boundaries and dislocations are clearly present, they do not significantly affect the τ_{eff} internal to the grains. After gettering (Fig. 4b) higher count rates and hence better global τ_{eff} are measured. However grain boundaries and dislocations have not improved noticeably.[19] Close inspection of grain boundaries bordering a high τ_{eff} grain reveals significant 'bleeding' compared to the sharper lines observed in Fig 4a. This would imply an increased recombination strength in these areas which is most noticeable in the black regions of high dislocation density.

A possible hypothesis for this is that dislocations have become decorated with impurities during high temperature processing, which the gettering was unable to affect, while the remainder of the grain has been 'cleaned' during the diffusion process. The decoration of these grain boundaries during phosphorus diffusion may explain the increased trapping observed in Fig. 1. In Fig. 4c, the distinction between grains is significantly reduced due to the passivation of grain boundaries. This reduction of recombination centres has increased the homogeneity of the sample which should translate into an improved open circuit voltage. However the potential global τ_{eff} of the material has

not been drastically increased. This is reflected in Fig. 3 where the "Gettered + Hydrogenated" samples show an average increase in τ_{eff} of approx. 20μs compared to their "Gettered" counterparts. As researchers have already shown that dislocation density and trap density are linked[13,18], and that traps can be passivated (Fig. 1)[14], Fig. 4c demonstrates that SiN induced hydrogenation can passivate grain boundaries and other dislocations[19] which are a primary source of carrier traps.

Conclusion

In this work we have examined how phosphorus gettering and SiN induced hydrogenation can improve the electronic properties of mc-Si. Examination of the [Fe_i] after each processing step, has revealed that phosphorus gettering is very effective at removing this fast diffusing impurity from the bulk of the grains. However our results do not support significant passivation of Fe_i by SiN hydrogenation. Area averaged trapping concentrations and PL imagery after each processing step, has revealed that carrier traps maybe caused by grain boundaries and lattice dislocations, which can be effectively passivated with SiN based hydrogenation. Average τ_{eff} of <10μs have been improved to >60μs through the combined use of phosphorus gettering and SiN hydrogenation. The phosphorus gettering has contributed to the improved τ_{eff} by removing τ_{eff} degrading metallic impurities, while the SiN hydrogenation has addressed other recombination sources such as lattice dislocations.

Acknowledgements

The authors would like to thank the Australian Research Council for funding this work. We would also like to thank Florence Chen for helping with the surface passivation of samples.

[1] O. Schultz, S. Glunz, S. Riepe, G. Willeke. High-Efficiency Solar Cells on Phosphorus Gettered Multicrystalline Silicon Substrates. *Progress in Photovoltics*, **14**, 711-719 (2006)

[2] C.J.J. Tool, P. Manshanden, A.R. Burgers, A.W. Weeber. Higher efficiency for thin multi crystalline silicon solar cells by improving the rear surface passivation. In *Proceeding 31st IEEE Conference*, 1324-1327, 2005

[3] A. Rohatgi and S. Narasimha. Design, fabrication, and analysis of greater than 18% efficient multicrystalline silicon solar cells. *Solar Energy Materials and Solar Cells*, Vol **48**, 187, 1997

[4] D. Macdonald, A. Cuevas, F. Ferrazza. Response to phosphorus gettering of different regions of cast multicrystalline silicon ingots. *Solid State Electronics*, Vol **43**, 575, 1999

[5] J. Boudaden, R. Monna, M. Loghmarti, J. C. Muller. Comparison of phosphorus gettering for different multicrystalline silicon. *Solar Energy Materials and Solar Cells*, Vol **72**, 381-387, 2002

[6] J.D. Moschner, J. Henze, J. Schmidt, and R. Hezel. High-quality surface passivation of silicon solar cells in an industrial-type inline plasma silicon nitride deposition system. *Progress in Photovoltaics*, **12**, 21 (2004)

[7] R. Sinton and A. Cuevas. Contactless determination of current-voltage characteristics and minority-carrier lifetimes in semiconductors from quasi-steady-state photoconductance data. *Applied Physics Letters*, **69**, 2510 (1996)

[8] T. Trupke, R. Bardos, M. Schubert, W. Warta. Photoluminescence imaging of silicon wafers. *Applied Physics Letters,* **89**, 044107 (2006)

[9] D. Macdonald and A. Cuevas, Trapping of minority carriers in multicrystalline silicon. *Applied Physics Letters,* **74**, 1710 (1999)

[10] J. Hornbeck and J. Haynes. Trapping of Minority Carriers in Silicon. I. P-Type Silicon. *Phys. Rev.* **77**, 311 (1955).

[11] P. Pohl, J. Schmidt, K. Bothe and R.Brendel. Mapping of trap densities and energy levels in semiconductors using a lock-in infrared camera technique. *Applied Physics Letters,* **87**, 142104 (2005)

[12] J. Schmidt, P. Pohl, K. Bothe, C. Schmiga, R. Krain and R. Brendel. Advanced Defect Characterisation Techniques in Crystalline Silicon based Photovoltaics. In *Proceeding 21st European Photovoltaic Energy Conference*, 2006

[13] M. Schubert, S. Riepe, S. Bermejo, W. Warta. Determination of spatially resolved trapping parameters in silicon with injection dependent carrier density imaging. *Journal of Applied Physics*, **99**, 114908 (2006)

[14] H. Dekkers, L. Carnel, G. Beaucarne. Carrier trap passivation in multicrystalline Si solar cells by hydrogen from SiNx:H layers. *Applied Physics Letters,* **89**, 013508 (2006)

[15] D. Macdonald, L. Geerligs, A. Azzizi. Iron detection in crystalline silicon by carrier lifetime measurements for arbitrary injection and doping. *Journal of Applied Physics*, **95** (3), 1021-1028 (2004)

[16] R. Sinton, T. Mankad, S. Bowden, N. Enjalbert. EVALUATING SILICON BLOCKS AND INGOTS WITH QUASI-STEADY-STATE LIFETIME MEASUREMENTS. In *Proceedings 19th European Photovoltaic Energy Conference*, 2004.

[17] A. Azzizi, L.J. Geerligs and D. Macdonald, HYDROGEN PASSIVATION OF IRON IN CRYSTALLINE SILICON. In *Proceeding 19th European Photovoltaic Energy Conference*, 2004

[18] P. Pohl, J. Schmidt, C. Schmiga and Rolf Brendel, Defect imaging in multicrystalline silicon using a lock-in infrared camera technique*, Journal of Applied Physics*, **101**(7), 073701 (2007)

[19] M. Rinio, M. Kaes, G. Hahn and D. Borchert, Hydrogen passivation of extended defects in multicrystalline silicon solar cells, *In Proceedings of the 21st European Photovoltaic and Solar Energy Conference*, 2006

[20] L.J. Geerligs, G. Coletti and D. Macdonald, On Accurate and Quantitative Measurements of Iron-Concentration in Multicrystalline Silicon by Iron-Boron Pair Dissociation*, In Proceedings of the 21st European Photovoltaic and Solar Energy Conversion*, 2006

[21] J. Henze, P. Pohl, C. Schmiga, M. Dhamrin, T. Saitoh, I. Yamaga and J. Schmidt, Millisecond area-averaged lifetimes in gallium doped multi-crystalline silicon, *In Proceedings of the 21st European Photovoltaic and Solar Energy Conversion*, 2006

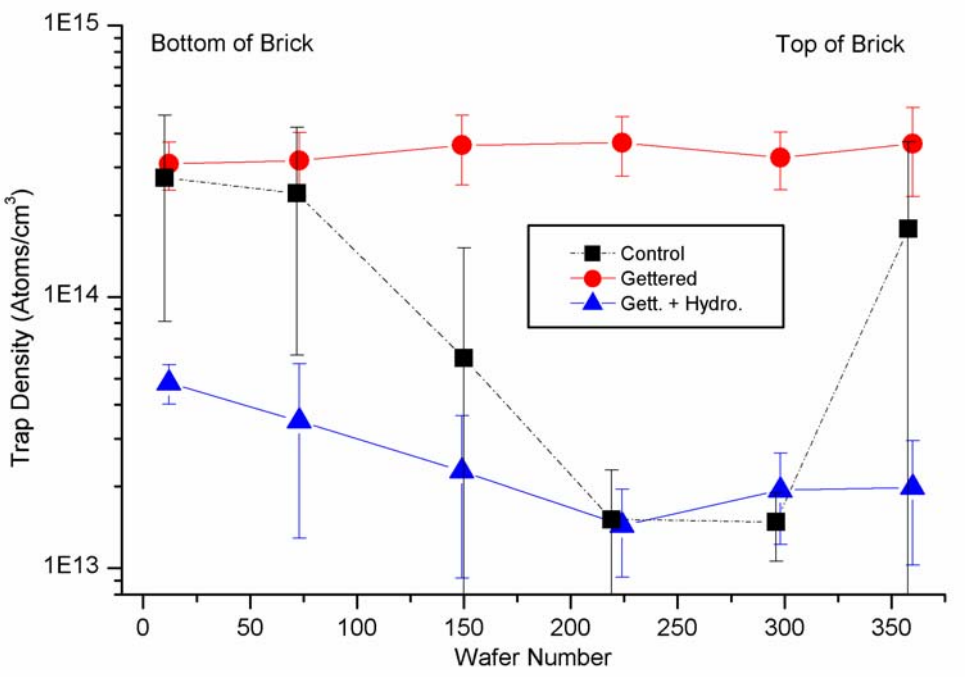

Figure 1 - Trap density of samples as a function of brick position. Lines are a guide to the eye. Error bars represent the standard deviation of the samples.

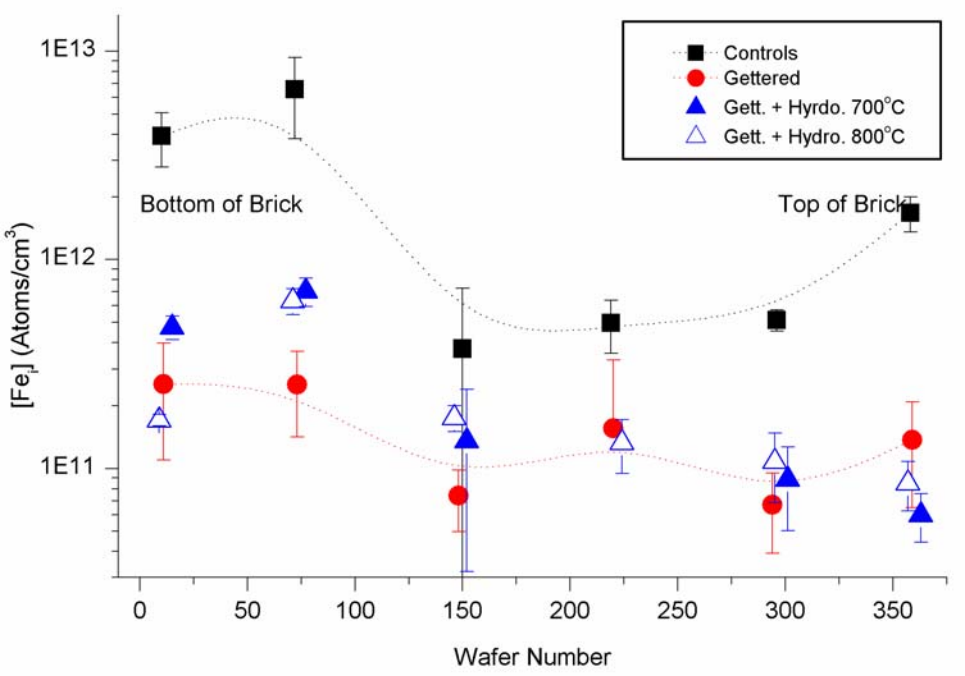

Figure 2 - Interstitial iron concentration as a function of brick position. Lines are a guide to the eye. Error bars represent the standard deviation of the samples.

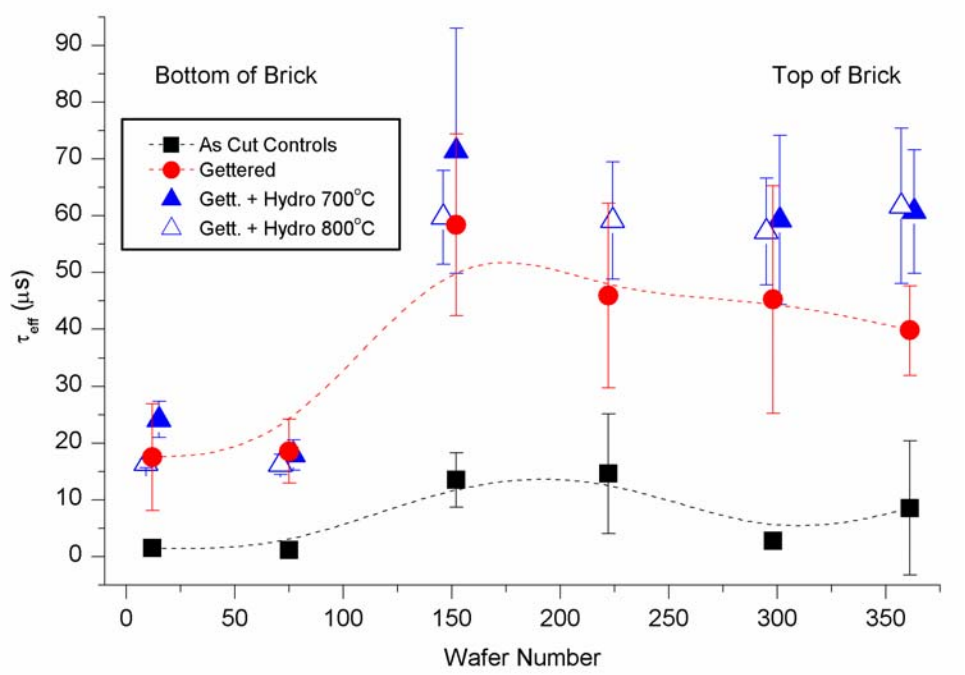

Figure 3 - Effective lifetime as a function of brick position. Lines are a guide to the eye. Error bars represent the standard deviation of the samples.

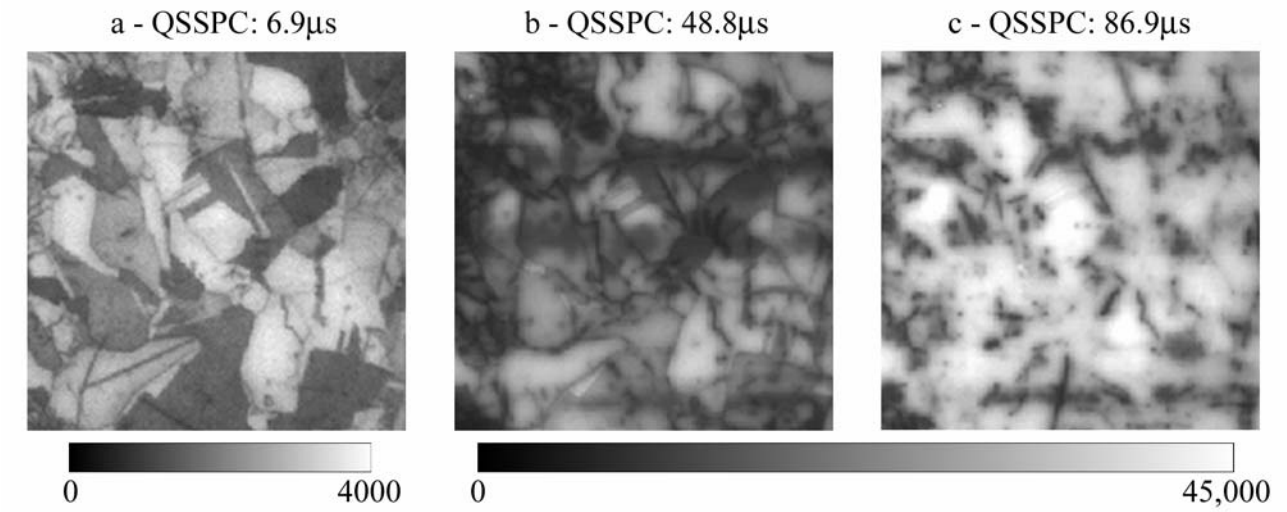

Figure 4 - PL images of (a) As Cut, (b) Gettered, (c) Gettered + Hydrogenated wafers. Colour bars represent the maximum count rates of the measurement